The Journal of Immunology

Cutting Edge: Bacillus Calmette–Guérin–Induced T Cells Shape *Mycobacterium tuberculosis* Infection before Reducing the Bacterial Burden

Jared L. Delahaye, Benjamin H. Gern, Sara B. Cohen, Courtney R. Plumlee, Shahin Shafiani, Michael Y. Gerner and Kevin B. Urdahl

J Immunol 2019; 203:807-812; Prepublished online 15 July 2019;
doi: 10.4049/jimmunol.1900108
http://www.jimmunol.org/content/203/4/807

The Journal of Immunology is published twice each month by
The American Association of Immunologists, Inc.,
1451 Rockville Pike, Suite 650, Rockville, MD 20852

Print ISSN: 0022-1767 Online ISSN: 1550-6606.

Cutting Edge

The Journal of Immunology

Cutting Edge: Bacillus Calmette–Guérin–Induced T Cells Shape *Mycobacterium tuberculosis* Infection before Reducing the Bacterial Burden

Jared L. Delahaye,*,† Benjamin H. Gern,* Sara B. Cohen,* Courtney R. Plumlee,* Shahin Shafiani,* Michael Y. Gerner,† and Kevin B. Urdahl*,†,‡

Growing evidence suggests the outcome of *Mycobacterium tuberculosis* infection is established rapidly after exposure, but how the current tuberculosis vaccine, bacillus Calmette–Guérin (BCG), impacts early immunity is poorly understood. In this study, we found that murine BCG immunization promotes a dramatic shift in infected cell types. Although alveolar macrophages are the major infected cell for the first 2 weeks in unimmunized animals, BCG promotes the accelerated recruitment and infection of lung-infiltrating phagocytes. Interestingly, this shift is dependent on CD4 T cells, yet does not require intrinsic recognition of Ag presented by infected alveolar macrophages. *M. tuberculosis*–specific T cells are first activated in lung regions devoid of infected cells, and these events precede vaccine-induced reduction of the bacterial burden, which occurs only after the colocalization of T cells and infected cells. Understanding how BCG alters early immune responses to *M. tuberculosis* provides new avenues to improve upon the immunity it confers. ***The Journal of Immunology*****, 2019, 203: 807–812.**

Bacillus Calmette–Guérin (BCG), the current tuberculosis (TB) vaccine, is effective at preventing disseminated disease in infants and young children (1). However, in most settings it provides little or no protection against adult pulmonary TB, the transmissible form of disease (2). Thus, despite widespread BCG immunization for nearly a century, *Mycobacterium tuberculosis* kills over 1.5 million people every year, more than any other single infectious agent (3). A better TB vaccine is urgently needed but attaining this goal has been surprisingly difficult (4). Furthermore, because BCG reduces childhood mortality, a new vaccine will likely be added to a regimen that includes BCG, rather than replace it (5). To develop a strategy that builds upon BCG-mediated protection, we must first understand how BCG shapes immunity to *M. tuberculosis*, especially during early stages of infection when protective immunity is established.

In mice, pulmonary *M. tuberculosis* burdens are equivalent between BCG-immunized and control mice until 2 weeks postinfection (6). The failure of BCG to impact the *M. tuberculosis* burden during the first 2 weeks of infection has been attributed to the delayed arrival of T cells in the lung (7). However, BCG-specific T cells have been shown to be present in the lungs (8) of immunized mice even prior to *M. tuberculosis* challenge, indicating that impaired T cell recruitment cannot fully account for the inability of BCG to induce early protection.

In this study, we used the mouse model to investigate the impact of BCG on the early immune response to *M. tuberculosis* infection. Our findings reveal unexpected roles for CD4 T cells in the following areas: 1) accelerating the translocation of *M. tuberculosis*–infected alveolar macrophages (AM) into the lung interstitium; 2) recruiting monocyte-derived macrophages (MDM); and 3) promoting the early transfer of *M. tuberculosis* from AM to other phagocytes. Despite these effects, a vaccine-induced reduction in the lung bacterial burden does not occur until colocalization of CD4 T cells with infected macrophages, which is delayed until 2 weeks postinfection, even in vaccinated animals.

Materials and Methods

Mice

ESAT-6 TCRtg (C7) mice were provided by Eric Pamer (9) and have been described previously. OTII mice were provided by Michael Gerner (University of Washington). C57BL/6 and MHC class II $(MHCII)^{-/-}$ mice were purchased from The Jackson Laboratory (Bar Harbor, ME). All mice were housed in specific pathogen–free conditions at Seattle Children's Research Institute. Experiments were performed in compliance with the Seattle Children's Research Institute Animal Care and Use Committee. Both male and female mice between the ages of 8–12 wk were used.

BCG immunization

BCG-Pasteur was cultured in Middlebrook 7H9 broth at 37°C to an OD of 0.2–0.5. Bacteria was diluted in PBS and 1×10^6 CFU in 200 μl

*Seattle Children's Research Institute, Seattle, WA 98109; †Department of Immunology, University of Washington School of Medicine, Seattle, WA 98109; and ‡Department of Pediatrics, University of Washington School of Medicine, Seattle, WA 98109

ORCIDs: 0000-0002-0142-5970 (B.H.G.); 0000-0002-7850-3498 (S.B.C.); 0000-0001-7142-4394 (C.R.P.); 0000-0001-5406-8308 (M.Y.G.).

Received for publication February 5, 2019. Accepted for publication June 25, 2019.

This work was supported by National Institutes of Health Grants 1R01AI134246 (to K.B.U.), 1R01AI076327 (to K.B.U.), U19AI135976 (to K.B.U.), 1R01AI134713 (to M.Y.G.), T32HD007233-37 (to B.H.G.), and T32GM007270-42 (to J.L.D.).

Address correspondence and reprint requests to Dr. Kevin B. Urdahl, Seattle Children's Research Institute, 307 Westlake Avenue North, Seattle, WA 98109. E-mail address: kevin.urdahl@seattlechildrens.org

The online version of this article contains supplemental material.

Abbreviations used in this article: AM, alveolar macrophage; BCG, bacillus Calmette–Guérin; LN, lymph node; MDM, monocyte-derived macrophage; MHCII, MHC class II; PMN, polymorphonuclear neutrophil; RT, room temperature; TB, tuberculosis; WT, wild-type.

www.jimmunol.org/cgi/doi/10.4049/jimmunol.1900108

was injected s.c. After immunization, mice were rested for 8 wk prior to *M. tuberculosis* infection.

Aerosol infections

Infections were performed with wild-type (WT) H37Rv *M. tuberculosis* or H37Rv transformed with an mCherry reporter plasmid (10). Mice were enclosed in a Glas-Col Inhalation Exposure System, and 50–100 CFU were deposited directly into the lungs.

Intratracheal and i.v. labeling

For intratracheal labeling, 30 min prior to sacrifice, mice were anesthetized with 20% isoflurane in propylene glycol (Thermo Fisher Scientific) and 0.25 μg of CD45.2 PE-Cy7 in 50 μl of PBS and was pipetted into the airway. For i.v. labeling, mice were anesthetized as above and infused with CD45.2 PE 10 min prior to sacrifice.

Lung cell isolation and Ab staining

Mouse lungs were homogenized in HEPES buffer with Liberase Blendzyme 3 (70 μg/ml; Roche) and DNaseI (30 μg/ml; Sigma-Aldrich) using a gentleMacs dissociator (Miltenyi Biotec). Lungs were incubated at 37°C for 30 min and then further homogenized with the gentleMacs. Cells were filtered through a 70-μm cell strainer and resuspended in RBC lysis buffer (Thermo Fisher Scientific) prior to a PBS wash. Cells were next incubated with 50 μl of Zombie Aqua viability dye (BioLegend) for 10 min at room temperature (RT). Viability dye was quenched with 100 μl of Ab mixture in 50% FACS buffer (PBS containing 2.5% FBS and 0.1% NaN_3)/50% Fc-block buffer. Staining was performed for 20 min at 4°C. Cells were washed with FACS buffer and fixed with 2% paraformaldehyde for 1 h prior to analysis on an LSR II flow cytometer (BD Biosciences). When stain sets contained tetramers, staining was performed for 1 h at RT. Ag85B (I-A(b) 280-294) and TB10.4 (K(b) 4-11) tetramers were obtained from the National Institutes of Health Tetramer Core Facility. Intracellular phospho-S6 (Ser235/236 2F9; Cell Signaling Technology) staining was performed for 1 h at RT with the FoxP3/Transcription Factor Staining Kit (Invitrogen).

Imaging

Mice were infected with H37Rv *M. tuberculosis*–mCherry and sacrificed at day 10 and day 14. Lungs were excised and submerged in BD Cytofix fixative solution diluted 1:3 with PBS for 24 h at 4°C. Lungs were washed two times in PBS and dehydrated in 30% sucrose for 24 h prior to OCT embedding and rapid freezing in a methylbutane–dry ice slurry. Twenty-micrometer sections were stained overnight at RT (with the following Abs: CD11c BV480; HL3 [BD Biosciences], CD11b BV510; M1/70 [BD Biosciences], CD45.2 Alexa Fluor 700; 104 [BioLegend], MHCII allophycocyanin-Fire750; M5/114.15.2 [BioLegend], Siglec-F BV421; E50-2440 [BD Biosciences], p-S6 Alexa Fluor 488; 2F9 [Cell Signaling Technology], CD3 CF633; 17A2, CD4 CF660C; RM4-5) and coverslipped with Fluoromount G mounting media (Southern Biotech). Images were acquired on a Leica SP8 confocal microscope, compensated for fluorophore spillover using LAS X (Leica) and analyzed with Imaris (Bitplane) and FlowJo (11). More details can be found in Supplemental Fig. 3.

T cell depletion and FTY720 treatment

To deplete T cells, mice were i.p. injected with 400 μg of anti-CD4 GK1.5 or anti-CD8 2.43 (Bio X Cell) in PBS at day 1, day 4, and day 10 relative to infection. To block T cell egress, mice were i.p. injected with 1 mg/kg FTY720 (Sigma-Aldrich) in water daily, starting 2 d prior to harvest.

Bone marrow chimeras

WT CD45.1/2 F1 mice were irradiated with 1000 rad and reconstituted with a 1:1 mixture of CD3-depleted (Miltenyi Biotec) CD45.1 B6.SJL:CD45.2 $MHCII^{-/-}$ bone marrow. At day 56 after reconstitution, mice were immunized with BCG.

Th1 polarization and adoptive transfers

CD4 T cells from ESAT-6–specific (C7) $CD90.1^+$ and OVA-specific (OTII) $CD45.1^+$ TCR transgenic mice were negatively enriched from spleens using EasySep magnetic microbeads (STEMCELL Technologies). T cells were Th1 polarized as follows: 1.6×10^6 transgenic T cells were cultured with 8.3×10^6 irradiated $CD3^-$ splenocytes. Five micrograms per milliliter of ESAT-6 or OVA peptide, 10 ng/ml IL-12, and 10 μg/ml of anti–IL-4 Ab (R&D Systems) were added at day 0. At day 3, cells were split 1:2, and 10 ng/ml IL-12 was added (R&D Systems). On day 5, Th1 cells were i.v. injected into mice infected with *M. tuberculosis* 10 d prior (Fig. 3C) or 35 d prior (Supplemental Fig. 2A).

Results and Discussion

BCG vaccination promotes M. tuberculosis *egress from AM early in infection*

To understand the effects of BCG immunization on early *M. tuberculosis* infection, we examined the pulmonary *M. tuberculosis* burdens in BCG-immunized and control mice. Consistent with prior reports (6, 7), lung burdens rose similarly in both groups through 2 wk (Fig. 1A). At day 15, the *M. tuberculosis* burden in the immunized group began to diverge and was reduced by one log by day 21. These findings are consistent with the idea that BCG-induced immunity is not initiated until the third week of *M. tuberculosis* infection.

We recently found that *M. tuberculosis* first infects AM before disseminating to other cells, including polymorphonuclear neutrophils (PMN) and MDM (12). As tissue-resident and recruited phagocytes have been shown to differ in their capacity to curb *M. tuberculosis* replication (13, 14), we next asked whether immunization alters the proportions of cell types that harbor infection. Consistent with the similar *M. tuberculosis* burdens at day 14, the numbers of cells harboring fluorescent *M. tuberculosis* (*M. tuberculosis*–mCherry) were also similar in each group (Fig. 1B). Surprisingly, even at this early phase, we observed a dramatic shift in the composition of infected cells. At day 14, by gating on $mCherry^+$ cells, we found that the proportion of *M. tuberculosis*–infected AM was significantly reduced in immunized animals compared with controls, with a corresponding increase in infected PMN and MDM (Fig. 1C, 1D). There was no effect on the infection of dendritic cells (Supplemental Fig. 1A). We confirmed these findings using confocal microscopy and quantitative histocytometry (11), wherein most *M. tuberculosis* was within $Siglec\text{-}F^+$ AM at day 14 in controls but within $CD11b^+$ $Siglec\text{-}F^-$ cells (primarily PMN and MDM) in immunized mice (Fig. 1E, 1F). As *M. tuberculosis* dissemination to PMN and MDM requires translocation of infected AM to the lung interstitium (12), we next assessed whether this translocation was accelerated in immunized mice. Indeed, intratracheal Ab administration, which specifically labels alveolar-localized cells (12), revealed significantly increased interstitial localization (label-negative) of infected AM in immunized mice at day 14 (Fig. 1G). Importantly, the changes in infected cell types was independent of changes in AM or PMN cellularity, as we found no differences in the numbers of these cells following immunization or infection (Supplemental Fig. 1B). Finally, immunization significantly enhanced MDM recruitment to the lung at day 14 (Fig. 1H), which was not observed at earlier time points or prior to infection (Supplemental Fig. 1B), suggesting that the accelerated recruitment of MDM in immunized mice begins between day 10 and day 14. Thus, although BCG does not impact the pulmonary *M. tuberculosis* burden in the first 2 wk of infection, it accelerates the translocation of infected AM from alveoli to the lung interstitium, MDM recruitment, and *M. tuberculosis* dissemination to PMN and MDM.

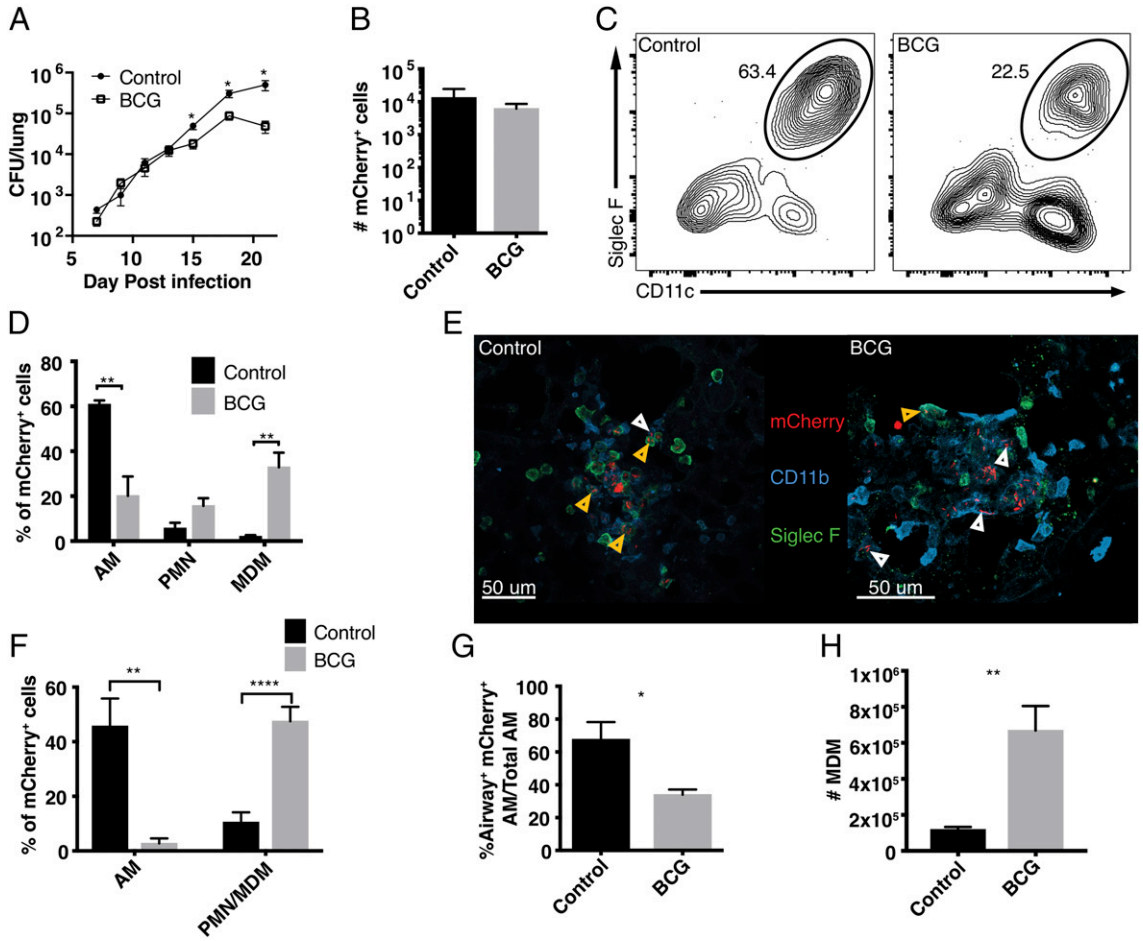

FIGURE 1. BCG vaccination promotes *M. tuberculosis* egress from AM early in infection. (**A**) *M. tuberculosis* burden in the lungs of mice that did or did not receive BCG (n = 4 mice per group per timepoint). (**B**) Total number of mCherry$^+$ lung cells at day 14 by flow cytometry (n = 4–5 mice per group). (**C**) Representative flow plot of the proportion of mCherry$^+$ cells identified as CD11c$^+$ Siglec-F$^+$ AMs at day 14. (**D**) Composition of mCherry$^+$ lung cells (AM: CD11c$^+$ Siglec-F$^+$; PMN: CD11b$^+$ Ly-6G$^+$; MDM: CD11b$^+$ CD64$^+$) at day 14 by flow cytometry (n = 4–5 mice per group). (**E**) Representative images of the lung (stained with Siglec-F BV421 and CD11b BV510) at day 14 showing infected Siglec-F$^+$ AM (orange arrows) and infected Siglec-F$^-$ CD11b$^+$ cells (white arrows). (**F**) Composition of mCherry$^+$ lung cells at day 14 by quantitative histocytometry (n = 6–8 infectious foci from two mice per group). (**G**) Ratio of airway label–positive–infected AM at day 14 (n = 5 mice per group). (**H**) Number of MDM in the lung at day 14 by flow cytometry (n = 4–5 mice per group). All experiments were performed at least two to three times. Single-group comparisons were performed by unpaired t test. Data are presented as mean ± SEM. $^*p < 0.05$, $^{**}p < 0.01$, $^{****}p < 0.0001$.

BCG accelerates the recruitment of Ag-specific T cells to the lung following M. tuberculosis *infection*

This unexpected impact of BCG on the early dynamics of infection led us to next investigate how immunization affects the kinetics of T cell recruitment to the lung. Before infection, Ag-specific CD4 (Ag85B) and CD8 (TB10.4) T cells could be identified in lung cell suspensions of immunized mice (Fig. 2A–C). Although ∼25% of the Ag85B-specific CD4 T cells were located in the lung parenchyma (as evidenced by their failure to stain with i.v. CD45 Ab), virtually all of the TB10.4-specific CD8 T cells resided in the vasculature (Fig. 2D). This difference is consistent with a recent report that lung CD4 T resident memory cells may be maintained for longer than CD8 T cells (15). Following infection, immunized mice had significantly more TB10.4-specific cells, as well as Ag85B-specific CD4 T cells, in the lung parenchyma than controls as early as day 10; by day 14 they contained >5-fold more (Fig. 2B, 2C). Thus, BCG induces a small population of lung-resident *M. tuberculosis*–specific CD4 T cells prior to infection. Postinfection, BCG accelerates the pulmonary accumulation of both CD4 and CD8 *M. tuberculosis*–specific T cells even before impacting the *M. tuberculosis* burden.

CD4 T cells are required for the accelerated transfer of M. tuberculosis *from AM to recruited phagocytes*

Given the presence of lung-resident *M. tuberculosis*–specific T cells in immunized mice prior to infection, we next determined whether T cells play a role in the accelerated transfer of *M. tuberculosis* from AM to other myeloid cells. CD4 or CD8 T cells were depleted from immunized mice beginning 1 d prior to *M. tuberculosis*–mCherry infection, and lung cells were assessed at day 14 (Supplemental Fig. 1C, 1D). In the absence of CD4 T cells, the accelerated transfer of *M. tuberculosis* from AM to PMN and MDM was partially reversed, whereas CD8 T cell depletion had no effect (Fig. 3A). Interestingly, the accelerated MDM recruitment (Fig. 1H) was also abolished by CD4 depletion (Fig. 3B). To assess whether antigenic recognition by CD4 T cells even in the absence of vaccination was sufficient to transfer *M. tuberculosis* infection from AM to other phagocytes, we adoptively transferred transgenic *M. tuberculosis* ESAT-6–specific CD4 T cells (C7),

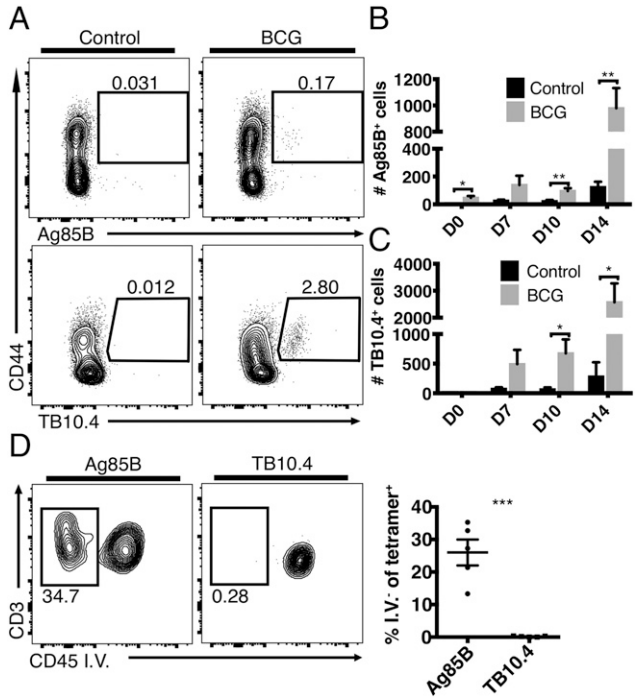

FIGURE 2. BCG accelerates the recruitment of Ag-specific T cells to the lung following *M. tuberculosis* infection. Time course of the number of tetramer-specific T cells in the lung. Mice received i.v. CD45 Ab prior to sacrifice. (**A**) Representative flow plots showing Ag85B-specific ($CD3^+CD4^+$) and TB10.4-specific ($CD3^+CD8^+$) T cells in the lungs of control and immunized mice prior to infection. The tetramer-positive cells in immunized mice are further gated on CD45 $i.v.^-$ to determine the proportion in the lung parenchyma. Total number of $i.v.^-$ Ag85B-specific (**B**) and TB10.4-specific (**C**) cells in the lungs of control and immunized mice ($n = 3$–5 mice per group per timepoint). (**D**) Proportion of tetramer-positive cells that are $i.v.^-$ in immunized mice at day 0 ($n = 5$ mice per group). All experiments were performed at least twice. Single-group comparisons were performed by unpaired *t* test. Data are presented as mean ± SEM. $^*p < 0.05$, $^{**}p < 0.01$, $^{***}p < 0.001$.

or OVA-specific CD4 T cells (OTII) as a control, into unimmunized mice that were infected with *M. tuberculosis* 10 d prior. Four days later (day 14) we observed that ESAT-6–specific but not OVA-specific T cells were sufficient to induce the transfer of infection out of AM (Fig. 3C), suggesting that Ag-specific CD4 T cell activation is needed to mediate this effect. Finally, we investigated whether direct recognition of *M. tuberculosis*–infected cells by CD4 T cells was required for the early dissemination out of the AM niche. WT (CD45.1): $MHCII^{-/-}$ (CD45.2) mixed bone marrow chimeras were generated, BCG immunized, and infected with *M. tuberculosis*–mCherry to test whether $MHCII^{-/-}$ AM, which cannot present Ag to CD4 T cells, would retain *M. tuberculosis* longer than WT AM. At day 14, BCG induced the accelerated transfer of *M. tuberculosis* from AM to other myeloid cells irrespective of intrinsic MHCII expression (Fig. 3D). Taken together, the results indicate that BCG-induced CD4 T cells promote the early transfer of *M. tuberculosis* from AM to other myeloid cells in a process that seems to require antigenic recognition but does not require direct cognate interactions between T cells and *M. tuberculosis*–infected AM. Our finding that CD4 T cells promote MDM recruitment to the lung, thereby providing new bacterial targets, may help explain the increased proportion of infected MDM in immunized animals. This recruitment likely relates to T cell production of cytokines, such as IFN-γ and TNF, which are known to trigger the release of chemokines that act on MDM (e.g., CCL2 and CXCL10) (16).

BCG-induced CD4 T cells are initially activated distal to the site of M. tuberculosis *infection*

Given that CD4 T cells seem to induce the transfer of infection independent of direct interactions with infected cells, we next sought to monitor T cell activation in the lung using phospho-S6 (p-S6), a ribosomal protein that is rapidly phosphorylated after TCR engagement and can be detected both by flow cytometry and confocal microscopy. Although previous work has shown that p-S6 specifically marks T cells that have recently engaged their TCR (peaking at 4 h and resolving within 24 h) under homeostatic conditions (17), we first confirmed this specificity in the context of *M. tuberculosis*–infected lungs by showing robust p-S6 expression by adoptively transferred TCR transgenic *M. tuberculosis*–specific (ESAT-6; C7) CD4 T cells compared with irrelevant TCR transgenic T cells (OVA-specific) (Supplemental Fig. 2A). Next, we examined p-S6 in the endogenous, polyclonal CD4 T cell population to monitor the kinetics and location of TCR signaling during early *M. tuberculosis* infection. Although there were very few $p\text{-}S6^+$ CD4 T cells in the lungs of either control or immunized mice prior to *M. tuberculosis* challenge, as measured by flow cytometry (Supplemental Fig. 2B), $p\text{-}S6^+$ CD4 T cells were readily identified in the vasculature of both unimmunized and immunized mice by day 10 and were present in higher numbers in the lung parenchyma of immunized mice compared with controls (Fig. 4A, Supplemental Fig. 2C). To assess the intrapulmonary location of these $p\text{-}S6^+$ cells, we performed confocal imaging and quantitative histocytometry (Supplemental Fig. 3). Consistent with our flow cytometry data, there were significantly more $p\text{-}S6^+$ cells in lung sections from immunized mice at day 10 (Fig. 4B, 4C), but, surprisingly, few of these cells were located near infected cells (Fig. 4B, 4G). Thus, although BCG induces early T cell recruitment and activation, at day 10 this occurs primarily in uninfected areas of the lung. This may be due to *M. tuberculosis* Ag export from infected to uninfected APCs (18) but could represent T cells that have recently trafficked from the lymph node (LN). To address this, we treated mice with FTY720, which blocks lymphocyte egress from lymphatic tissue, for 48 h prior to analysis (Supplemental Fig. 2D). Although FTY720 treatment almost completely eliminated $p\text{-}S6^+$ CD4 T cells in the lung vasculature at day 10, the number of $p\text{-}S6^+$ T cells in the lung parenchyma ($i.v.^-$) was only partially reduced (Fig. 4D). These results suggest that most of the recently activated T cells in the vasculature and a subset of those in the lung parenchyma had recently egressed from the LN. However, some of the $p\text{-}S6^+$ cells in the lung parenchyma at day 10 were likely activated in the lungs. Taken together, these results indicate that the activation of BCG-induced CD4 T cells, which occurs distal to sites of infection, shapes immunity to *M. tuberculosis* challenge earlier than previously appreciated by facilitating the pulmonary recruitment of MDM and accelerating the transfer of *M. tuberculosis* from AM to other myeloid cells. This transfer likely influences the ability of the BCG-immunized host to control *M. tuberculosis*, as prior studies have shown that tissue-resident versus recruited macrophages differ profoundly in their capacity

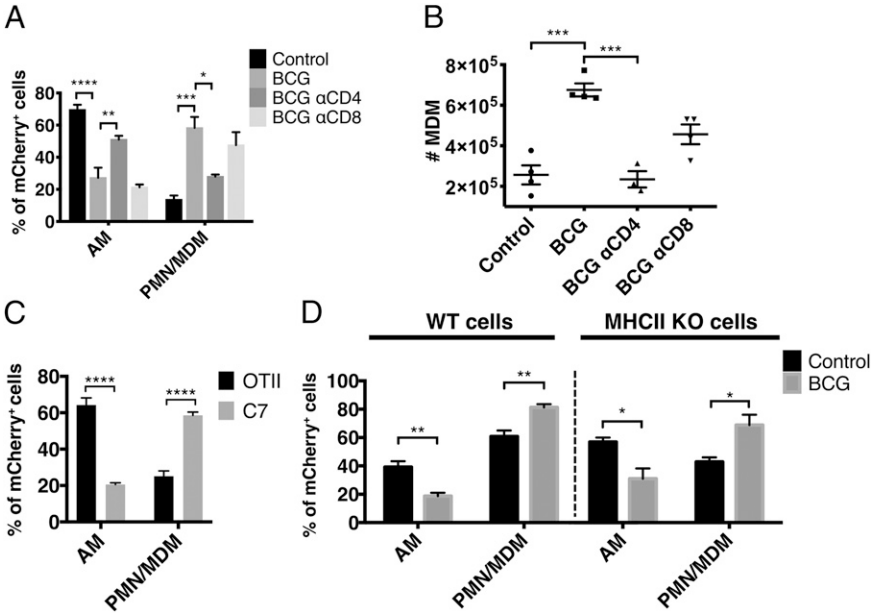

FIGURE 3. CD4 T cells are required for the accelerated transfer of *M. tuberculosis* from AM to recruited phagocytes. (**A**) Composition of mCherry$^+$ cells in control, immunized, and T cell–depleted immunized mice at day 14 (n = 4 mice per group). (**B**) Total number of MDM as in (A). (**C**) Composition of mCherry$^+$ cells at day 14 in mice that received either OTII or C7 Th1 cells at day 10 (n = 5 mice per group). (**D**) Composition of CD45.1$^+$ WT (left) and CD45.2$^+$ knockout (KO) (right) mCherry$^+$ cells in control and immunized mixed bone marrow chimeras at day 14 (n = 3–4 mice per group). All experiments were performed at least twice. Single-group comparisons were performed by unpaired t test (C and D) and multiple-group comparisons by one-way ANOVA (A and B). Data are presented as mean ± SEM. $^*p < 0.05$, $^{**}p < 0.01$, $^{***}p < 0.001$, $^{****}p < 0.0001$.

to control *M. tuberculosis* replication (13, 14). Future studies are needed to elucidate the overall impact on protection because the settings in which distinct macrophage types mediate enhanced immunity remain unclear.

Interestingly, BCG-induced CD4 T cells only begin to curb *M. tuberculosis* replication at day 14, when they finally colocalize with cells harboring *M. tuberculosis*, as evidenced by the identification of many p-S6$^+$ cells in the lung parenchyma and at sites of infection compared with controls (Fig. 4E–G). This is consistent with the finding that optimal immunity against *M. tuberculosis* requires direct interactions between Ag-specific CD4 T cells and infected cells (19). Importantly, in contrast to our findings at day 10, at day 14, FTY720 had no effect on the number of p-S6$^+$ CD4 T cells recovered from the lung parenchyma of BCG-immunized mice (Fig. 4H), suggesting that almost all of these T cells were activated in the lungs rather than the LN. Why do T cells and *M. tuberculosis*–infected cells not colocalize earlier? The AM is the first cell

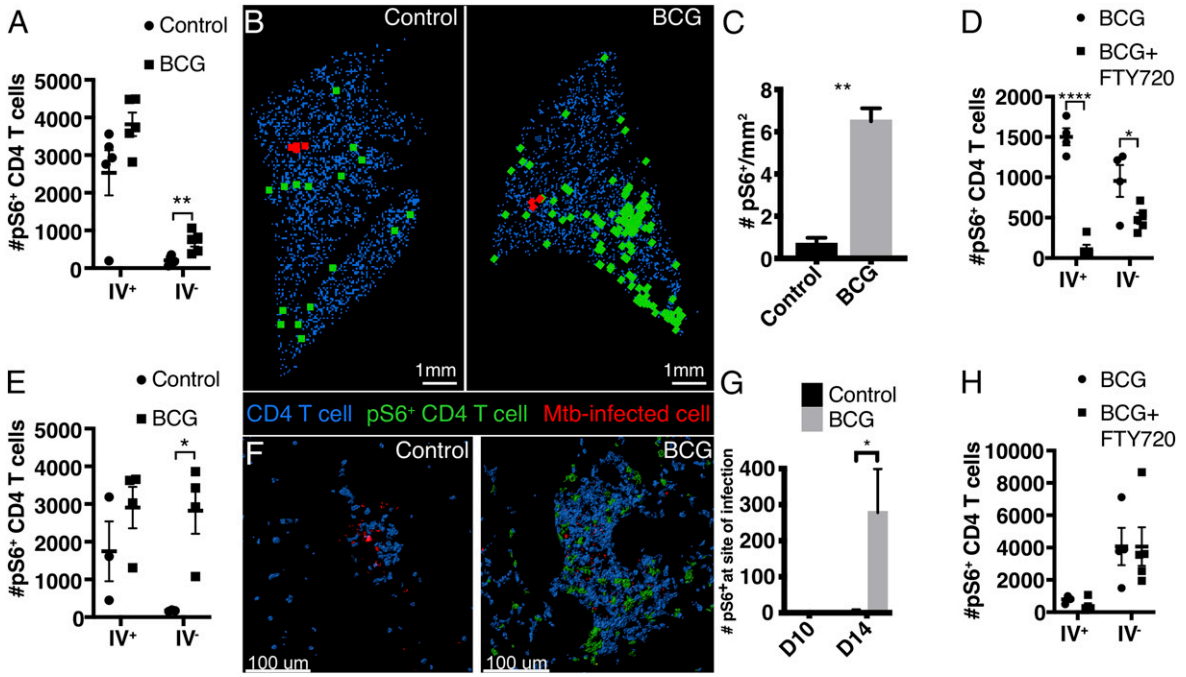

FIGURE 4. BCG-induced CD4 T cells are initially activated distal to the site of *M. tuberculosis* infection. Total numbers of i.v.$^+$ and i.v.$^-$ p-S6$^+$ CD4 T cells at day 10 (**A**) and day 14 (**E**). Quantitative histocytometry was used to identify the location of CD4 T cells (blue) and p-S6$^+$ CD4 T cells (green) relative to infected cells (red) in lung sections at day 10 (**B**) and sites of infection at day 14 (**F**). The confocal images used to generate these plots were stained with CD3 CF633, CD4 CF660, and p-S6 Alexa Fluor 488. (**C**) Number of p-S6$^+$ CD4 T cells per square millimeter of lung at day 10 as determined by quantitative histocytometry (n = 2–3 mice per group). Total numbers of i.v.$^+$ and i.v.$^-$ p-S6$^+$ CD4 T cells at day 10 (**D**) and day 14 (**H**) in immunized mice treated with FTY720. (**G**) Number of p-S6$^+$ CD4 T cells within 80 μm of an infected cell (n = 6–8 sections from two mice per group). This cutoff was based on the limit of IFN-γ diffusion within tissue (20). Single-group comparisons were performed by unpaired t test. Data are presented as mean ± SEM. $^*p < 0.05$, $^{**}p < 0.01$, $^{****}p < 0.0001$.

type to become infected and remains the primary infected cell type for at least a week (12). During this time, the immune system appears largely unaware of the looming threat, as few MDM or PMN are recruited to the lung. The recent finding that AM infection is noninflammatory and poorly induces chemokines may help explain the covert nature of early infection (21). Identifying vaccination approaches that enable T cells to colocalize with *M. tuberculosis*–infected AM may promote earlier *M. tuberculosis* control. Together, these results demonstrate that BCG immunization shapes early T cell and myeloid cell responses in the lung and new vaccine strategies should consider the dynamics of both these compartments.

Acknowledgments

We thank Peter Andersen, Joshua Woodworth, and Rasmus Mortensen for critical feedback of the manuscript as well as Bridget Alexander, the flow cytometry core, and vivarium staff for technical assistance.

Disclosures

The authors have no financial conflicts of interest.

References

1. Trunz, B. B., P. Fine, and C. Dye. 2006. Effect of BCG vaccination on childhood tuberculous meningitis and miliary tuberculosis worldwide: a meta-analysis and assessment of cost-effectiveness. *Lancet* 367: 1173–1180.
2. Mangtani, P., I. Abubakar, C. Ariti, R. Beynon, L. Pimpin, P. E. Fine, L. C. Rodrigues, P. G. Smith, M. Lipman, P. F. Whiting, and J. A. Sterne. 2014. Protection by BCG vaccine against tuberculosis: a systematic review of randomized controlled trials. *Clin. Infect. Dis.* 58: 470–480.
3. World Health Organization. 2018. *Global Tuberculosis Report 2018.* World Health Organization, Geneva.
4. Tameris, M. D., M. Hatherill, B. S. Landry, T. J. Scriba, M. A. Snowden, S. Lockhart, J. E. Shea, J. B. McClain, G. D. Hussey, W. A. Hanekom, et al; MVA85A 020 Trial Study Team. 2013. Safety and efficacy of MVA85A, a new tuberculosis vaccine, in infants previously vaccinated with BCG: a randomised, placebo-controlled phase 2b trial. *Lancet* 381: 1021–1028.
5. Roth, A. E., L. G. Stensballe, M. L. Garly, and P. Aaby. 2006. Beneficial nontargeted effects of BCG--ethical implications for the coming introduction of new TB vaccines. *Tuberculosis (Edinb.)* 86: 397–403.
6. Mollenkopf, H. J., M. Kursar, and S. H. Kaufmann. 2004. Immune response to postprimary tuberculosis in mice: Mycobacterium tuberculosis and Miycobacterium bovis bacille Calmette-Guérin induce equal protection. *J. Infect. Dis.* 190: 588–597.
7. Ronan, E. O., L. N. Lee, P. C. Beverley, and E. Z. Tchilian. 2009. Immunization of mice with a recombinant adenovirus vaccine inhibits the early growth of *Mycobacterium tuberculosis* after infection. *PLoS One* 4: e8235.
8. Santosuosso, M., S. McCormick, X. Zhang, A. Zganiacz, and Z. Xing. 2006. Intranasal boosting with an adenovirus-vectored vaccine markedly enhances protection by parenteral *Mycobacterium* bovis BCG immunization against pulmonary tuberculosis. *Infect. Immun.* 74: 4634–4643.
9. Gallegos, A. M., E. G. Pamer, and M. S. Glickman. 2008. Delayed protection by ESAT-6-specific effector CD4+ T cells after airborne *M. tuberculosis* infection. *J. Exp. Med.* 205: 2359–2368.
10. Cosma, C. L., O. Humbert, and L. Ramakrishnan. 2004. Superinfecting mycobacteria home to established tuberculous granulomas. *Nat. Immunol.* 5: 828–835.
11. Gerner, M. Y., W. Kastenmuller, I. Ifrim, J. Kabat, and R. N. Germain. 2012. Histo-cytometry: a method for highly multiplex quantitative tissue imaging analysis applied to dendritic cell subset microanatomy in lymph nodes. *Immunity* 37: 364–376.
12. Cohen, S. B., B. H. Gern, J. L. Delahaye, K. N. Adams, C. R. Plumlee, J. K. Winkler, D. R. Sherman, M. Y. Gerner, and K. B. Urdahl. 2018. Alveolar macrophages provide an early Mycobacterium tuberculosis niche and initiate dissemination. *Cell Host Microbe* 24: 439–446.e4.
13. Huang, L., E. V. Nazarova, S. Tan, Y. Liu, and D. G. Russell. 2018. Growth of *Mycobacterium tuberculosis* in vivo segregates with host macrophage metabolism and ontogeny. *J. Exp. Med.* 215: 1135–1152.
14. Cambier, C. J., K. K. Takaki, R. P. Larson, R. E. Hernandez, D. M. Tobin, K. B. Urdahl, C. L. Cosma, and L. Ramakrishnan. 2014. Mycobacteria manipulate macrophage recruitment through coordinated use of membrane lipids. *Nature* 505: 218–222.
15. Turner, D. L., M. Goldklang, F. Cvetkovski, D. Paik, J. Trischler, J. Barahona, M. Cao, R. Dave, N. Tanna, J. M. D'Armiento, and D. L. Farber. 2018. Biased generation and in situ activation of lung tissue-resident memory CD4 T cells in the pathogenesis of allergic asthma. *J. Immunol.* 200: 1561–1569.
16. Murray, H. W., A. D. Luster, H. Zheng, and X. Ma. 2016. Gamma interferon-regulated chemokines in *Leishmania* donovani infection in the liver. *Infect. Immun.* 85: ee00824-16.
17. Sauer, S., L. Bruno, A. Hertweck, D. Finlay, M. Leleu, M. Spivakov, Z. A. Knight, B. S. Cobb, D. Cantrell, E. O'Connor, et al. 2008. T cell receptor signaling controls Foxp3 expression via PI3K, Akt, and mTOR. *Proc. Natl. Acad. Sci. USA* 105: 7797–7802.
18. Srivastava, S., P. S. Grace, and J. D. Ernst. 2016. Antigen export reduces antigen presentation and limits T cell control of *M. tuberculosis. Cell Host Microbe* 19: 44–54.
19. Srivastava, S., and J. D. Ernst. 2013. Cutting edge: direct recognition of infected cells by CD4 T cells is required for control of intracellular *Mycobacterium tuberculosis* in vivo. *J. Immunol.* 191: 1016–1020.
20. Müller, A. J., O. Filipe-Santos, G. Eberl, T. Aebischer, G. F. Späth, and P. Bousso. 2012. CD4+ T cells rely on a cytokine gradient to control intracellular pathogens beyond sites of antigen presentation. *Immunity* 37: 147–157.
21. Rothchild, A. C., G. S. Olsen, J. Nemeth, L. M. Amon, D. Mai, E. S. Gold, A. H. Diercks, and A. Aderem. 2019. Alveolar macrophages generate a noncanonical NRF2-driven transcriptional response to *Mycobacterium tuberculosis* in vivo. *Sci. Immunol.* In press.